

Flies compensate for unilateral wing damage through modular adjustments of wing and body kinematics.

Florian T. Muijres, Nicole A. Iwasaki, Michael J. Elzinga, Johan M. Melis & Michael H. Dickinson
Interface Focus

ELECTRONIC SUPPLEMENTARY MATERIAL

Table S1: Average normalized forces in the world reference frame and torques in the body reference frame of all simulated flies with wing damage using the *normal* and *WDR* kinematics, and percentages of contribution to damage control of the relevant kinematics parameters. A control contribution of 100% denotes full weight support for F_z/mg and zero force or torque production for all other degrees of freedom. Negative values denote a detrimental contribution to flight control, and absolute contributions of 25% or more are shown in bold.

	F_x/mg	F_y/mg	F_z/mg	T_x/mgl	T_y/mgl	T_z/mgl
<i>Normal kinematics</i>	-0.03	0.04	0.78	0.058	-0.008	-0.004
<i>WDR kinematics</i>	-0.04	0.01	0.95	0.012	-0.015	0.025
<i>Stroke angle</i>	17%	11%	4%	53%	-12%	244%
↓↑	↓	↓	↓	↑	↑	↑
<i>Deviation angle</i>	-1%	-101%	17%	36%	-129%	656%
↓↑	↓	↓	↓	↑	↑	↑
<i>Rotation angle</i>	-20%	-78%	-17%	17%	-80%	-216%
↓↑	↓	↓	↓	↑	↑	↑
<i>Body roll angle</i>	0%	246%	11%	0%	0%	0%
↓↑	↓	↓	↓	↑	↑	↑
<i>Wingbeat frequency</i>	-7%	-10%	139%	-27%	131%	-26%
<i>All parameters</i>	-12%	68%	154%	79%	-90%	657%

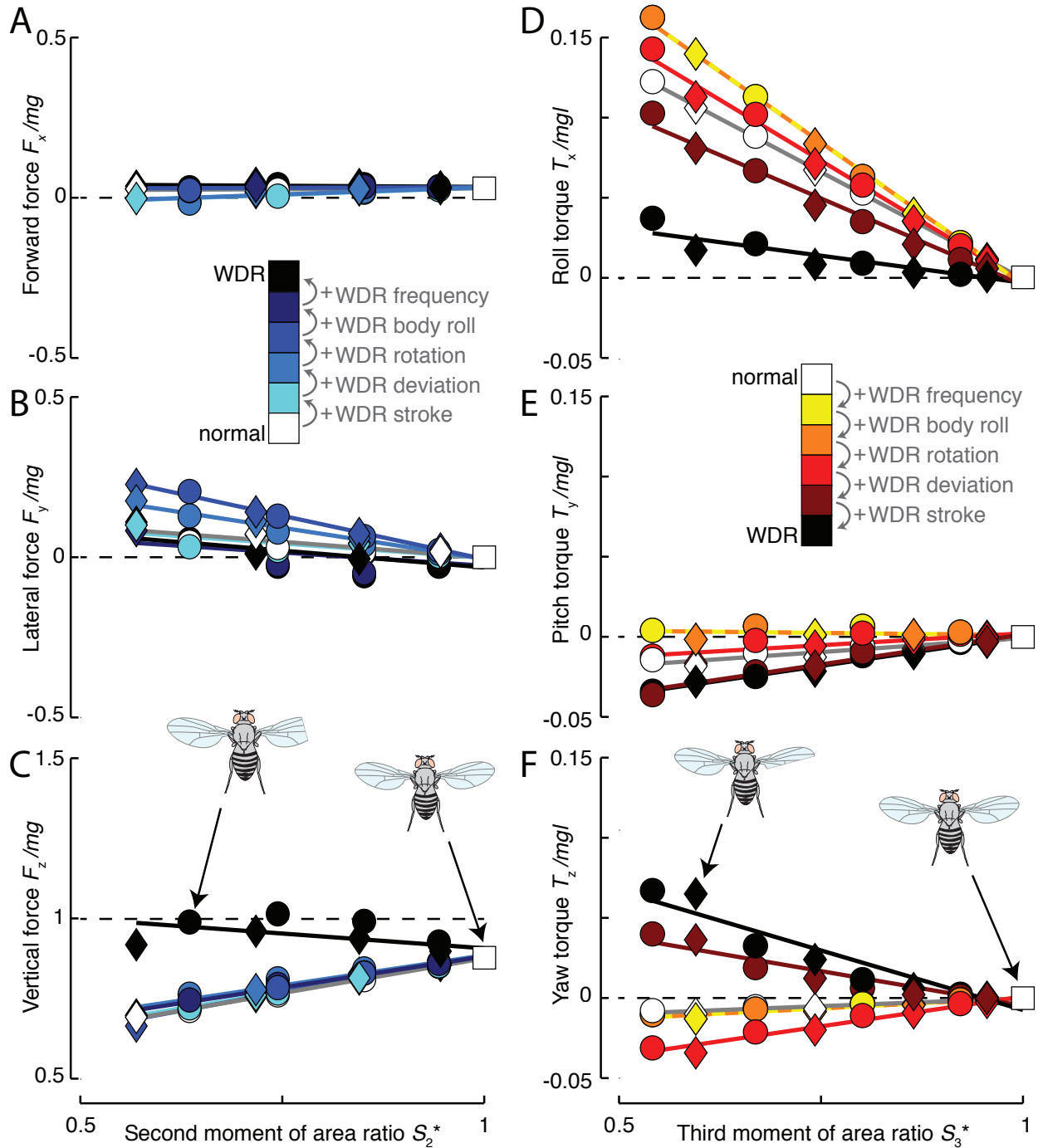


Figure S1. Wingbeat-average aerodynamic forces in the world reference frame (A-C) and torques in the body reference frame (D-F) produced by simulated flies with variable amounts of wing damage, and when cumulatively replacing the different normal kinematics parameters with the WDR kinematics. The sequence of kinematics replacement is according to the legends in panel A and E for forces and torques, respectively). Results from flies with a spanwise cut wing are indicated by diamonds, flies with cordwise wingcuts are indicated by circles, and squares are for intact flies.

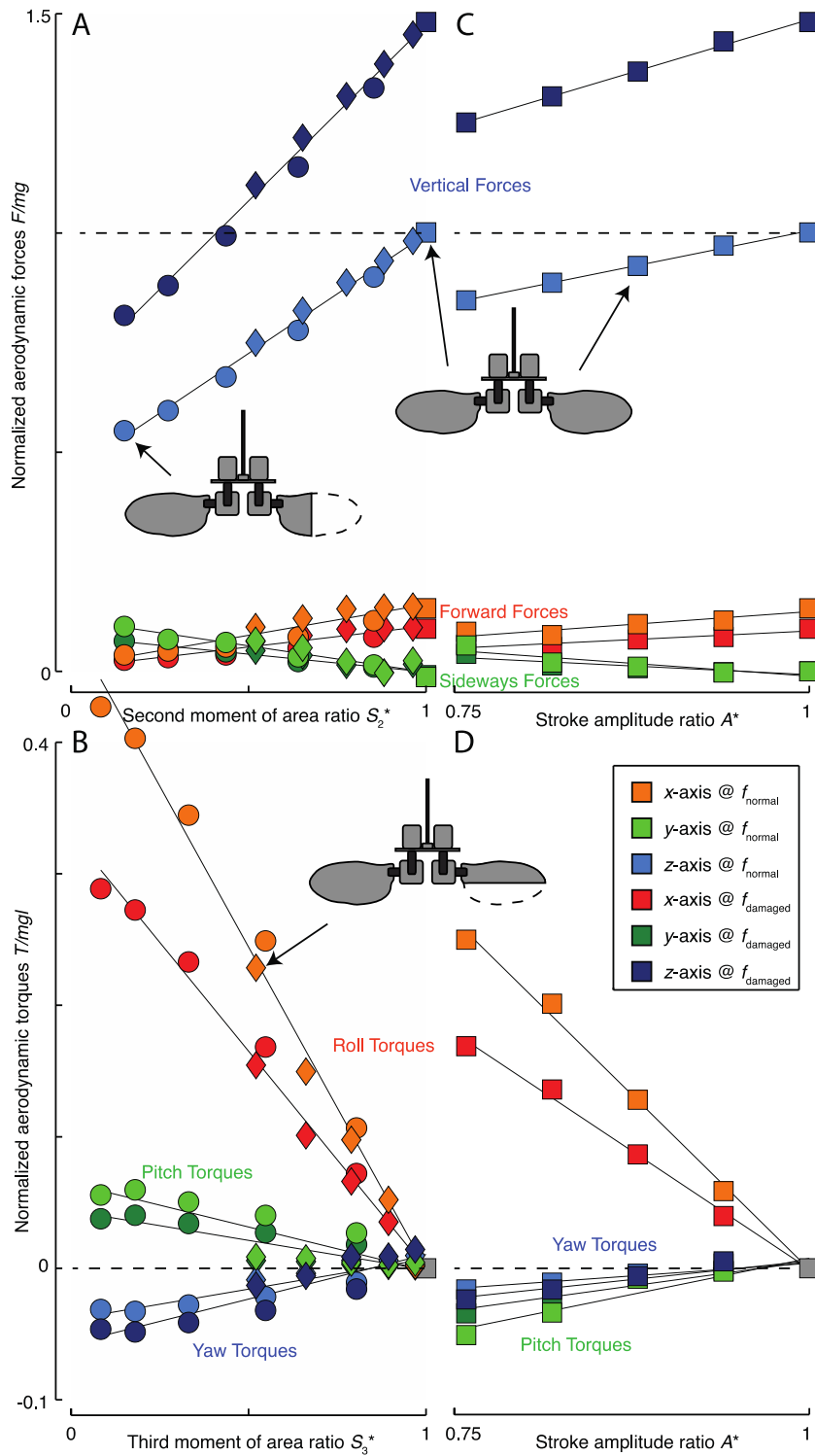


Figure S2. Forces and torques produced by a robotic fruit fly with the right wing damaged (A,B), or with an intact right wing with varying wing stroke amplitude (C,D). (A) Aerodynamic forces scale linearly with the normalized second moment of area, S_2^* , irrespective of the type of damage (cordwise or spanwise). (B) Likewise, aerodynamic torques scale linearly with the third moment of area ratio, S_3^* . Wingbeat kinematics in (A,B) consisted of the normal pattern of *D. hydei* with undamaged wings (Fig. 1D). (C,D) Aerodynamic forces and torques scale linearly with the normalized stroke amplitude, A^* . Here, the left wing followed the normal wingbeat kinematics, while the right wing flapped with variable stroke amplitude (Fig. 1D).

Different colors indicate forces and torques about the three body axes at both the normal wingbeat frequency of undamaged flies (f_{normal}) and mean flap frequency of flies with a damaged wing ($f_{damaged}$), see legend. Squares show data from a robotic fly with both wings intact, circles show data for a robot fly with a cordwise cut wing, and diamonds show data for the robot with a spanwise cut wing.

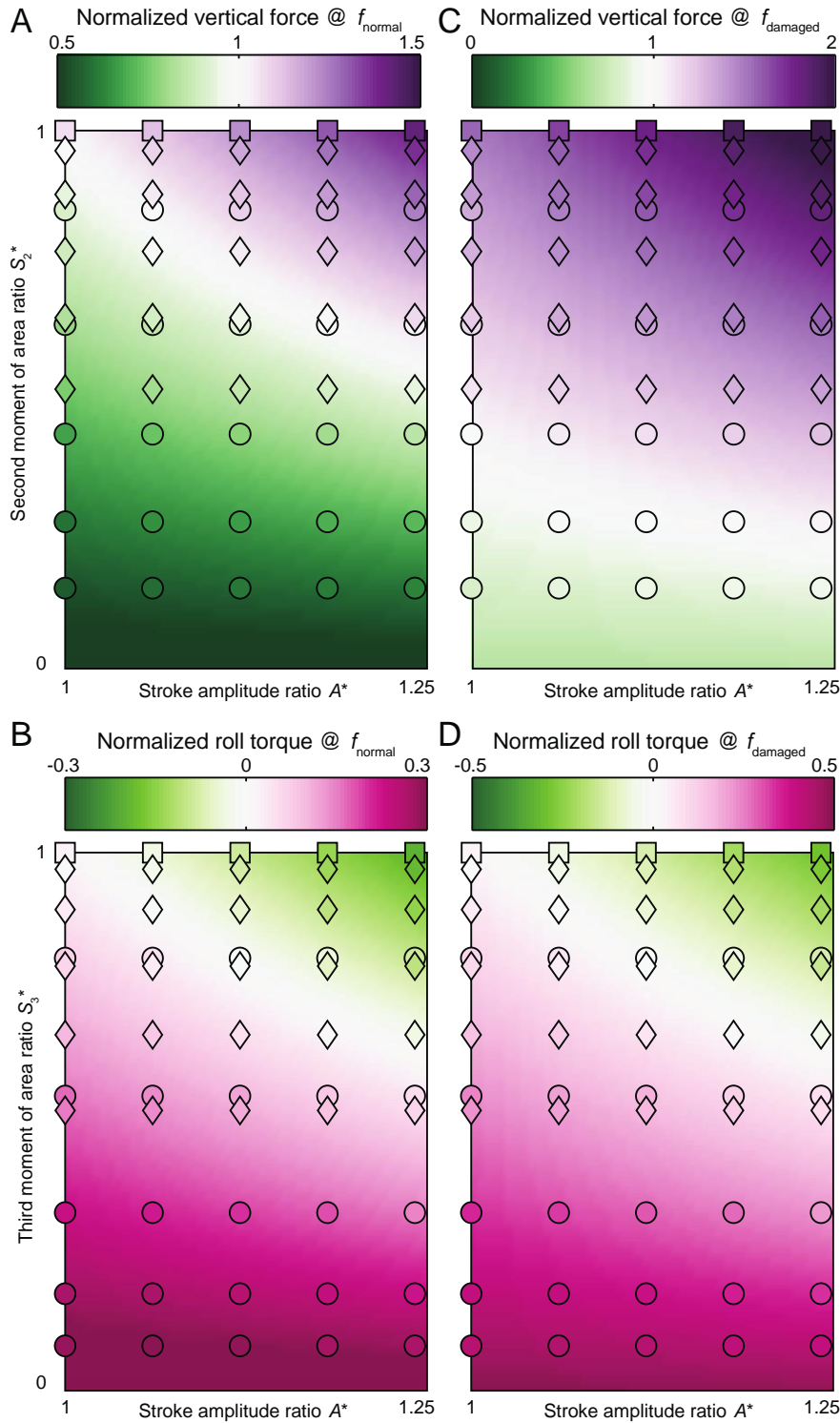


Figure S3. Aerodynamic forces and torques produced by the robotic fruit fly with a right wing with variable stroke amplitudes and variable damage (the left wing was left intact and flapped with a constant stroke amplitude). All data points were color coded with vertical force (A,C) or roll torque (B,D) according to the color-bar above each panel.

The color-coded surfaces show linear fits (including interactions) through the data points (Eq. 9). The left column (A,B) shows the results of the robotic fruit fly flying at the wingbeat frequency of *D. hydei* with undamaged wings (f_{normal}), whereas the right column (C,D) shows data for wings beating at the mean wingbeat frequency of

flies with a damaged wing (f_{damaged}). In all panels, squares represent data of a fly robot with undamaged wings, diamonds are of the robot with a trailing edge wing cut and circles show data for the robotic fly with a damaged wingtip.

Video S1: High-speed video of a flying fruit fly with spanwise wing damage. The flight sequence corresponds to the morphology and kinematics data in Fig. 2E-G. The fly was filmed from above at 7500 frames per second, but is replayed at 300x slower speed.

Video S2: High-speed video of a flying fruit fly with spanwise wing damage. The flight sequence corresponds to the morphology and kinematics data in Fig. 2E-G. The fly was filmed from the front at 7500 frames per second, but is replayed at 300x slower speed.

Video S3: High-speed video of a flying fruit fly with chordwise wing damage. The flight sequence corresponds to the morphology and kinematics data in Fig. 2H-J. The fly was filmed from above at 7500 frames per second, but is replayed at 300x slower speed.

Video S4: High-speed video of a flying fruit fly with chordwise wing damage. The flight sequence corresponds to the morphology and kinematics data in Fig. 2H-J. The fly was filmed from the side at 7500 frames per second, but is replayed at 300x slower speed.

Dataset S1: Wing morphology and flight kinematics of all free flight experiments on flies with unilateral wing damage. Data are stored in a Matlab (MathWorks Inc., Natick, MA, USA) dataset format (mat-file).

Dataset S2: wing shape parameters, wingbeat kinematics and force and torque output from robotic fly experiments. Data are stored in a Matlab (MathWorks Inc., Natick, MA, USA) dataset format (mat-file).

Dataset S3: smoothing spline parameters for body roll and wingbeat frequency as a function of wing damage ($\phi_{\text{WDR}}(\mathcal{A}^+)$ and $f_{\text{WDR}}(\mathcal{A}^+)$, respectively); Fourier series coefficients of $\text{MOD}(\phi_{\text{damaged}})$, $\text{MOD}(\gamma_{\text{damaged}})$, $\text{MOD}(\alpha_{\text{damaged}})$, $\text{MOD}(\phi_{\text{intact}})$, $\text{MOD}(\gamma_{\text{intact}})$, $\text{MOD}(\alpha_{\text{intact}})$, as defined in Eq. 3; expressions of $b_{\mathcal{A}^+}$, $b_{\mathcal{A}^{\text{intact}}}$ and $b_{\mathcal{A}^{\text{damaged}}}$ at both f_{damaged} and f_{normal} as defined in Eq. 2 and Eq. 8; The surface fit coefficients for aerodynamic vertical force and roll torque as a function of wing damage and wingbeat amplitude of the robotic fruit fly model, at both f_{damaged} and f_{normal} and as defined in Eq. 9. Data are stored in a Matlab (MathWorks Inc., Natick, MA, USA) dataset format (mat-file).